Macromolecular Design of Novel Sulfur-Containing Copolyesters with Promising Mechanical Properties

M. Gigli,[1] N. Lotti,[1] M. Gazzano,[2] L. Finelli,[1] A. Munari[1]

[1]*Dipartimento di Ingegneria Civile, Ambientale e dei Materiali, Università di Bologna, Via Terracini 28, 40131 Bologna, Italy*
[2]*Istituto per la Sintesi Organica e la Fotoreattività, CNR, Via Selmi 2, 40126 Bologna, Italy*

Received 20 October 2011; accepted 18 January 2012
DOI 10.1002/app.36856
Published online in Wiley Online Library (wileyonlinelibrary.com).

ABSTRACT: The miscibility of poly(butylene succinate) (PBS)/poly(butylene thiodiglycolate) (PBTDG) blends was investigated by DSC technique. PBS and PBTDG were completely immiscible in as blended-state, as evidenced by the presence of two T_gs at −34 and −48°C, respectively. The miscibility changes upon mixing at elevated temperature: the original two phases merged into a single one because of transesterification reactions. Poly(butylene succinate/thiodiglycolate) block copolymers, prepared by reactive blending of the parent homopolymers, were studied to investigate the effects of transesterification reactions on the molecular structure and solid-state properties. ^{13}C-NMR analysis evidenced the formation of copolymers whose degree of randomness increased with mixing time. Thermal characterization results showed that all the samples were semicrystalline, with a soft rubbery amorphous phase and a rigid crystal phase whose amount decreased by introducing BTDG units into the PBS chain ($20 \leq \chi_c \leq 41$). Lastly, the mechanical properties were found strictly related to crystallinity degree (χ_c), the random copolymer, exhibiting the lowest elastic modulus ($E = 61$ MPa) and the highest deformation at break (ε_b (%) = 713). © 2012 Wiley Periodicals, Inc. J Appl Polym Sci 000: 000–000, 2012

Key words: poly(butylene succinate); thiodiglycolic acid; reactive blending; transesterication reactions; block copolymers; thermal properties; mechanical properties; X-ray diffraction

INTRODUCTION

Because the human body is a complex system, a large variety of materials with different characteristics are needed to fulfil all conceivable applications. Today, homopolymers of resorbable aliphatic polyesters including poly(L-lactide) and poly(ε-caprolactone) are most frequently used in biomedical applications, but the need of new materials with improved properties is still large. For example, in the case of soft tissue engineering applications, the availability of biodegradable polymeric materials to produce scaffolds characterized by elastomeric mechanical behavior suitable to withstand cyclic deformation and to transfer mechanical stress to cultured cells is low.[1–8] More precisely, taking into account that biodegradable porous scaffolds have to fulfil several functions to work effectively in a tissue engineering application, the material has to be characterized by proper mechanical properties and degradation profile, while being biocompatible and non toxic. One of the most promising way of creating such materials is copolymerization, which enables the material's degradation and mechanical characteristics to be tailored, because the copolymers inherit the properties of the homopolymers. On this ground, recently, our group has performed quite extensive work: several series of novel block copolyesters of poly(butylene succinate) (PBS), promising for uses as environmentally biodegradable thermoplastics, as well as bioabsorbable/biocompatible medical materials, were prepared and characterized from the molecular and solid-state point of view,[9–15] with particular attention devoted to the mechanical properties. In the case of block poly(butylene/diethylene succinate) and poly(butylene/triethylene succinate) copolyesters, wetting behavior, hydrolytic degradation profile, and biocompatibility of these new materials were also checked and correlated to the molecular architecture.[11,14] The most recently synthesized system is represented by poly(butylene succinate/diglycolate) block copolymers, where the butylene diglycolate comonomeric unit differs from that of PBS for the presence in the diacid subunit of an ether-oxygen atom.[15] We decided to carry on the research by replacing the ether-oxygen atom with a sulfur one, which, as well known, is characterized by larger dimensions and is less electronegative. These chemical characteristics should render the resulting sulfur-containing copolymers less rigid. At first, we prepared the poly(butylene thiodiglycolate)

Correspondence to: N. Lotti (nadia.lotti@.unibo.it).

(PBTDG) homopolymer by the usual two-stage polycondensation procedure; then block copolyesters (PBSPBTDG) were obtained by reactive blending of PBS previously synthesized[15] and PBTDG.

Polymer blending is also an attractive alternative route for producing new polymeric materials with desirable properties being versatile, simple, and inexpensiveness. Unfortunately, most polymers are thermodynamically immiscible, giving rise to physical mixtures that often are characterized by poor mechanical properties. In the case of polyesters, transesterications reactions in both the molten and the solid state can be promoted converting the blends first to block copolymers and lastly to random ones. The resultant initial block and eventual random copolymers usually exhibit enhanced mutual miscibility when compared with the original nonreacted components,[16–19] and consequently, the final properties of the material are significantly improved. It is worth noting that reactive blending is a simple and versatile solvent-free method, which permits to modulate the final properties of the material simply by varying mixing time.

The aim of this work is, therefore, to prepare a new family of copolymers with mechanical properties suitable for applications in soft tissue engineering, characterized by a controlled degrees of randomness enabling easy tailoring of the materials properties.

EXPERIMENTAL

Products

Dimethylsuccinate (DMS), dimethylthiodiglycolate (DMTDG), 1,4-butanediol (BD), and titanium tetrabutoxide ($Ti(OBu)_4$) (Aldrich) were reagent grade products; DMS, DMTDG, and BD were used as supplied, whereas $Ti(OBu)_4$ was distilled before use.

Synthesis of homopolymer PBTDG

PBTDG was synthesized in bulk starting from dimethylthiodiglycolate and 1,4-butanediol (using a 20% mol excess of the glycol on respect of DMTDG), using $Ti(OBu)_4$ as catalyst (about 0.2 g of $Ti(OBu)_4$/kg of polymer). The synthesis was carried out in a 250-mL stirred glass reactor, with a thermostatted silicon oil bath; temperature and torque were continuously recorded during the polymerization. The polymer was prepared according to the usual two-stage polymerization procedure. In the first stage, under pure nitrogen flow, the temperature was raised to 180°C and kept constant until more than 90% of the theoretical amount of methanol was distilled off (about 2 h). In the second stage, the pressure was reduced to about 0.1 mbar to facilitate the removal of the glycol in excess, and the temperature was raised to 200°C; the polymerization was carried out until a torque constant value was measured. The chemical structure of the homopolymer synthesized is the following:

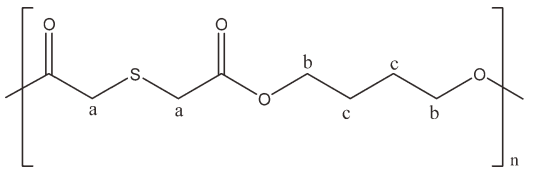

PBTDG

Solution cast blends

Solution cast blends of PBS and PBTDG were prepared by solution mixing in chloroform (4 wt % polymer solution) of weighed amounts of the two blend components for each composition at room temperature. Films were obtained by solvent evaporation and kept in a vacuum oven at room temperature for at least 30 days before testing, to eliminate completely the residual solvent. Throughout this work, the resulting blends are denoted as ScbPBSPBTDGX, where X is the mol percentage of PBTDG in the blends.

Synthesis of poly(butylene succinate/thiodiglycolate) copolyesters

Poly(butylene succinate/thiodiglycolate) copolyesters were obtained by melt mixing of PBS obtained previously[15] and PBTDG. The two homopolymers were mixed in a 1 : 1 molar ratio in a 200-mL glass reactor at 225°C under dry nitrogen atmosphere to prevent hydrolytic degradation. During the process, samples were taken from the reactor at different reaction times (10, 45, 120, 180, and 240 min) and cooled in air. Copolymer formation was catalyzed by the residual titanium tetrabutoxide introduced in the polymerization of PBS and PBTDG. The copolyesters obtained and analyzed in this work will be indicated as PBSPBTDGt, where t is the mixing time expressed in min.

Film preparation

Films of PBSPBTDG copolymers were obtained by compression molding the polymers between Teflon plates, with an appropriate spacer, at a temperature $T = T_m + 40$°C, for 2 min under a pressure of 2 ton/m^2 (Carver C12, laboratory press). The obtained films were 0.2 ± 0.02 mm thick.

NMR spectroscopy

The polymer structure and composition were determined by means of ^{1}H-NMR spectroscopy, whereas

the distribution of the comonomeric sequences along the polymer chain was evaluated by ^{13}C-NMR spectroscopy. The samples were dissolved in chloroform-d solvent with 0.03% (v/v) tetramethylsilane added as an internal standard. ^{1}H-NMR spectra were recorded at room temperature for solutions with a polymer concentration of 0.5 wt % (a relaxation delay of 0 s, an acquisition time of 1 s and up to 100 repetitions). ^{13}C-NMR spectra were obtained using 5 wt % solutions and a full decoupling mode with a NOE effect (a relaxation delay of 1 s, an acquisition time of 1 s and up to 700 repetitions). A Varian INOVA 400 MHz instrument was used for the measurements.

Gel-permeation chromatography

Molecular weight data were obtained by gel-permeation chromatography at 30°C using a 1100 Hewlett Packard system equipped with PL gel 5μ MiniMIX-C column (250/4.6 length/i.d., in mm). A refractive index detector was used. In all cases, chloroform was used as eluent with a 0.3 mL/min flow, and sample concentrations of about 2 mg/mL were applied. A calibration curve was obtained using several polystyrene standards in the range of molecular weight 2,000–100,000.

Wide-angle X-ray diffraction measurements

X-ray diffraction (XRD) patterns of polymeric films were carried out by using a PANalytical X'PertPro diffractometer equipped with a fast solid state X'Celerator detector and a copper target (λ = 0.15418 nm). Data were acquired in the 5–60° 2θ interval, by collecting 100 sat each 0.10° step. The indices of crystallinity (χ_c) were evaluated from the XRD profiles by the ratio between the crystalline diffraction area (A_c) and the total area of the diffraction profile (A_t), $X_c = A_c/A_t$. The crystalline diffraction area has been obtained from the total area of the diffraction profile by subtracting the amorphous halo. The amorphous was modelled as a bell-shaped peak baseline. The noncoherent scattering was taken into consideration.

The crystal sizes perpendicular to 1 1 0 planes were calculated by using the Scherrer method, from the broadening at half the maximum intensity of the peak at 22.7° (2θ) (shape factor = 1.0; instrumental broadening taken in the due account).[20]

Stress–strain measurements

Stress–strain measurements were performed with an Instron 4465 tensile testing machine equipped with a 100 N load cell, on rectangular films (5 mm wide and 0.2 mm thick). The gauge length was 20 mm, and the cross-head speed was 5.0 mm/min. Load–displacement curves were obtained and converted to stress strain curves. Tensile elastic modulus was determined from the initial linear slope of the stress–strain curve. At least, six replicate specimens were run for each sample, and the results were provided as the average value ± standard deviation.

Thermal analysis

TG measurements

Thermogravimetric analysis was carried out both in air and under nitrogen atmosphere using a Perkin Elmer TGA7 apparatus (gas flow: 30 mL/min) at 10°C/min heating rate up to 900°C. The procedure suggested by the supplier was followed for the temperature calibration of the equipment. This method is based on the change of the magnetic properties of two metal samples (nickel and perkalloy) at their Curie points (354.0 and 596.0°C, respectively).

DSC measurements

Calorimetric measurements were carried out by means of a Perkin Elmer DSC7 instrument equipped with a liquid sub ambient accessory and calibrated with high purity standards (indium and cyclohexane). With the aim of measuring the glass transition and the melting temperatures of the polymers under investigation, the external block temperature control was set at −120°C, and weighed samples of c.a. 10 mg were encapsulated in aluminum pans and heated to about 40°C above fusion temperature at a rate of 20°C/min (first scan), held there for 3 min, and then rapidly quenched (about 100°C/min) to −80°C. Finally, they were reheated from −80°C to a temperature well above the melting point of the sample at a heating rate of 20°C/min (second scan). The glass-transition temperature T_g was taken as the midpoint of the heat capacity increment Δc_p associated with the glass-to-rubber transition. The melting temperature (Tm) and the crystallization temperature (Tc) were determined as the peak value of the endothermal and the exothermal phenomena in the DSC curve, respectively. When multiple endotherms were observed, the highest peak temperature was taken as Tm. The specific heat increment Δc_p, associated with the glass transition of the amorphous phase, was calculated from the vertical distance between the two extrapolated baselines at the glass transition temperature. The heat of fusion (ΔHm) and the heat of crystallization (ΔHc) of the crystal phase were calculated from the total areas of the DSC endotherm and exotherm, respectively. To determine the crystallization rate under nonisothermal conditions, the samples were heated at 20°C/min to about 40°C above fusion

TABLE I
Molecular Characterization Data

Polymers	M_n	D	BS (mol %) ^{13}C-MNR	L_{BS}	L_{BTDG}	b
PBS[a]	51200	2.3	100			
PBDTG	40900	2.2	0			
PBSPBTDG10	42000	2.2	50.3	/	/	0.0
PBSPBTDG45	45200	2.1	49.6	10.4	9.9	0.2
PBSPBTDG120	48500	2.4	49.7	4.4	3.8	0.49
PBSPBTDG180	48800	2.5	50.2	3.0	2.6	0.73
PBSPBTDG240	49400	2.1	53.4	2.2	1.8	1.01

[a] From Ref. 15.

temperature, kept there for 3 min and then cooled at 5°C/min. The temperature corresponding to the maximum of the exothermic peak in the DSC cooling-curve (T_{cc}) can be correlated to the crystallization rate.

Repeated measurements on each sample showed excellent reproducibility.

RESULTS AND DISCUSSION

PBTDG homopolymer

At room temperature, the as-prepared polyester is a light brown colored rubber. The sample was kept at ambient temperature for 2 weeks before characterization. As it can be noted from Table I reported below, PBTDG is characterized by a relatively high molecular weight, indicating that appropriate synthesis conditions and a good polymerization control were obtained. To have an understanding into the chemical structure, the ^{1}H-NMR investigation was performed. The spectrum was found to be consistent with the expected structure, the chemical shift assignments (δ, ppm) being the following: PBTDG: δ = 4,16 (t, 4 H^b); δ = 3,38 (s, 4 H^a); δ = 1,75 (m, 4 H^c) (see the chemical structure reported in the Experimental Section). Subsequently, the polyester was subjected to thermogravimetric analysis, and the temperature corresponding to 5% weight loss ($T_{5\%}$) and the temperature corresponding to the maximum weight loss rate (T_{max}) were determined and collected in Table III. As evidenced in Figure 1, the weight loss takes place practically in one-step and is 100%. From the comparison between the TGA curves of PBTDG and that of PBS added for comparison,[15] one can see that the latter is more thermally stable. As a matter of fact, as documented in the literature,[21] the introduction of ethero atoms along the polymer chains affects the thermal stability, in particular favoring the thermooxidative processes of decomposition. Moreover, taking into account that among the various degradation mechanisms proposed to shed light on the thermal degradation reactions occurring in polyesters, the random cleavage of covalent bonds of the polymeric chains can be invoked, the higher stability of PBS with respect of PBTDG can be explained on the basis of the higher energy of the C—C bond with respect to C—S one.

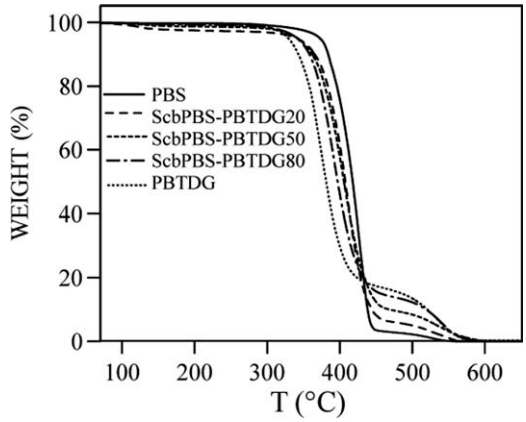

Figure 1 Thermogravimetric curves of PBS (from Ref. 15), PBTDG, and solution cast blends ScbPBS-PBTDGSX in air (heating rate: 10°C/min).

As regards the calorimetric results, the phase behavior of the two parent homopolymers is opposite: as a matter of fact, PBS is semicrystalline,[15] whereas PBTDG is amorphous. T_g values of the two polymers cannot be easily compared because after melt quenching PBS is still highly semicrystalline and is well known crystallinity acting like crosslinking raises T_g. Anyway, the high difference between the two T_gs values indicates that PBTDG is characterized by a lower glass transition temperature than

TABLE II
Thermal Characterization Data of PBS, PBTDG, and ScbPBS-PBTDGSX Solution Cast Blends

Blends	$T_{5\%}$ (°C)	T_{max} (°C)	2nd Scan T_g (°C)	ΔC_p (J/g°C)	T_m (°C)	ΔH_m (J/g)	X_c (%)
PBS[a]	393	428	−34	0.104	113	63	32
PBTDG	344	373	−48	0.520	–	–	–
ScbPBS-PBTDG20	357	389	−48 −34	0.14 0.06	115	45.6	29
ScbPBS-PBTDG50	368	402	−48 −35	0.29 0.09	115	29.3	29
ScbPBS-PBTDG80	374	408	−49 −34	0.50 0.08	114	12.1	30

[a] From Ref. 15.

PBS. To explain this result, the larger dimension of sulfur atoms with respect to the carbon ones has to be taken into consideration: as a matter of fact S—C bonds longer than the C—C ones form, making the polymer chains more flexible.

Solution cast blends

The as-prepared blends of PBS and PBTDG were opaque because of the crystallinity generated during the storage at room temperature (more than 2 weeks), due to the semicrystalline nature of PBS blend component. Preliminarily, the solution cast blends were subjected to thermogravimetric analysis to evaluate the thermal stability as a function of composition. From the thermogravimetric curves in air, the temperature corresponding to 5% weight loss ($T_{5\%}$) and the temperature corresponding to the maximum weight loss rate (T_{max}) were determined and collected in Table II.

The weight loss is 100%, analogously to the two parent homopolymers (see Fig. 1). As far as the thermal stability is concerned, it was found to depend on composition, being lower as PBTDG content increases. However, all the samples are characterized by a good thermal stability, the temperature of initial decomposition $T_{5\%\,w.loss}$ ranging from 357 to 374°C (see Table II).

As is well known, the miscibility of polymer blends is frequently judged by the analysis of their glass transition. In fact, in blends as well as in block copolymers, the presence of a single glass transition at a temperature intermediate with respect to the T_gs of the pure components, suggests complete miscibility; on the contrary, the appearance of two T_gs indicates immiscibility or partial miscibility of the components. In particular, the presence of two glass transitions, at temperatures corresponding to those of the pure homopolymers, is a clear evidence of no miscibility. Lastly, the observation of two glass transition phenomena whose position changes with composition proves the existence of two mixed phases, each one able to accommodate molecules of the second component (partial miscibility). Therefore, to better evaluate the miscibility in the amorphous phase, the DSC scans after melt quenching have been analyzed. As evident from the data collected in Table II, all the blends examined are semicrystalline, being characterized by a conspicuous melting endotherm, the temperature of the melting peak not changing appreciably with respect to that of PBS.

As far as the glass transition phenomenon is concerned, as evidenced in Figure 2, where, as an example, the second calorimetric scan of ScbPBS-PBTDG80 is shown, no evidence of compatibility is obtained by calorimetric measurements: in fact, two distinct glass transitions, with constant temperatures

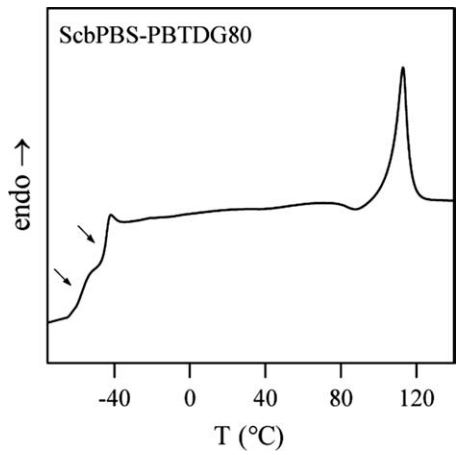

Figure 2 Calorimetric curve of PBS-PBTDG80 solution cast blend after melt quenching (2nd scan).

corresponding to those of the pure blend components are evident. In conclusion, in ScbPBS-PBTDGX solution cast blends no miscibility at all was found, and therefore, the system analyzed formed a biphasic system over the whole composition range, with the phases consisting of the two pure homopolymers.

Poly(butylene succinate/thiodiglycolate) copolymers

To obtain block copolymers, equimolar amounts of PBS and PBTDG were melt mixed at high temperature. Several preliminary runs carried out at different reaction temperatures were performed (165, 215, 225, and 233°C) to optimize mixing conditions. The best temperature turned out to be 225°C, which was adopted to prepare the copolymers under investigation. At RT, the as-prepared copolymers are opaque and light brown colored solids.

PBSPBTDGt samples, together with the parent homopolymers for comparison, are listed in Table I along with molecular characterizations data. As it can be seen, all the copolyesters are characterized by relatively high molecular weights, intermediate between those of the parent homopolymers PBS and PBTDG. This result indicates that no relevant thermal degradation occurs during the mixing. Looking into more detail the data, a slight increase of molecular weight with the mixing time is observed. This result is not surprising taking into account that transesterification reactions prevail on chain scission reactions at long mixing times, in the range of time employed.

The chemical structure of all copolyesters was determined by ^{1}H-NMR spectroscopy. As an example, the ^{1}H-NMR spectrum of PBSPBTDG120 is shown in Figure 3, together with the chemical shift assignments. In all cases, the spectra were found to be consistent with the expected structures. The

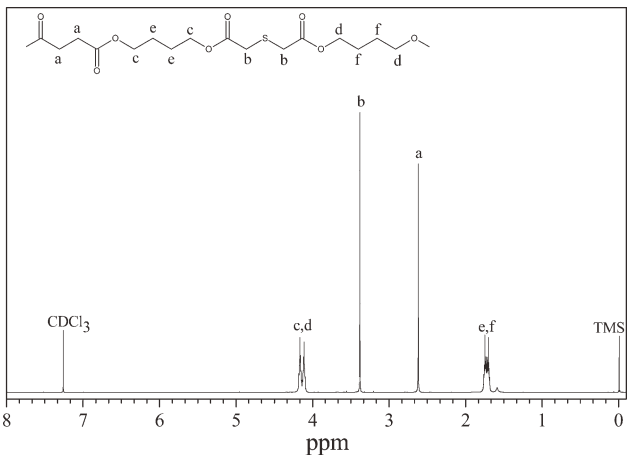

Figure 3 ^{1}H-NMR spectrum of PBSPBTDG12 copolymer.

copolymer composition was calculated from the relative areas of the ^{1}H-NMR resonance peak of the **a** aliphatic proton of the succinic subunit located at 2.61 ppm and of the **b** protons of the thiodiglycolic subunit at 3.38 ppm. From the data of Table I, it can be seen that in all cases the actual molar composition is very close to the feed one.

Because the ^{1}H-NMR resonance peaks of interest (**e** and **f**) in evaluating the progress of transesterication reactions are not sufficiently resolved, ^{13}C-NMR measurements were performed to study the structural changes. In particular, the region between $\delta = 64.1$ and $\delta = 65.5$ ppm (where the signals due to the carbon atoms of the 1,4-butanediol glycol subunit are located) is of special interest to evaluate the extent of the transesterification reactions occurring during the mixing at high temperature between PBS and PBTDG (see the peaks labelled as **c** and **h** in Fig. 4).

As evident from Figure 5, where the region between 64.1 and 65.5 ppm is reported for some copolymers, the ^{13}C-NMR spectrum of PBSPBTDG10 (corresponding $t_{mix} = 10$ min) is the mere additive spectra of PBS and PBTDG homopolymers, indicating that no appreciable chemical reactions took place during their mixing at 225°C. In fact, if transesterification reactions between PBS and PBTDG occurred, new peaks should appear due to the mixed sequences (see Fig. 5).

As a matter of fact, in the copolymers PBSPBTDG obtained after mixing times longer than 10 min, two new peaks, due to the mixed sequences, develop. As it can be seen from Figure 5, the intensity of these last increases with mixing time, indicating that the transesterification reactions proceeded.

Information on the arrangement of the comonomeric units in the chain can be deduced by the degree of randomness b, which can be determined by ^{13}C-NMR spectroscopy. It has to be emphasized that b is equal to 1 for random copolymers, equal to 2 for alternate copolymers, closed to zero for a mixture of two homopolymers and $0 < b < 1$ for block copolymers.

The calculation of b has been carried out taking into consideration the resonance peaks of the carbon atoms of the succinic subunit (**c** and **h)**, so that it can be expressed[22]:

$$b = P_{S-TDG} + P_{TDG-S} \quad (1)$$

where $P_{S\text{-}TDG}$ and $P_{TDG\text{-}S}$ are the probability of finding a *S* unit next to a *TDG* unit and the probability of finding *TDG* unit next to a *S* unit, respectively. The two probabilities can be expressed as:

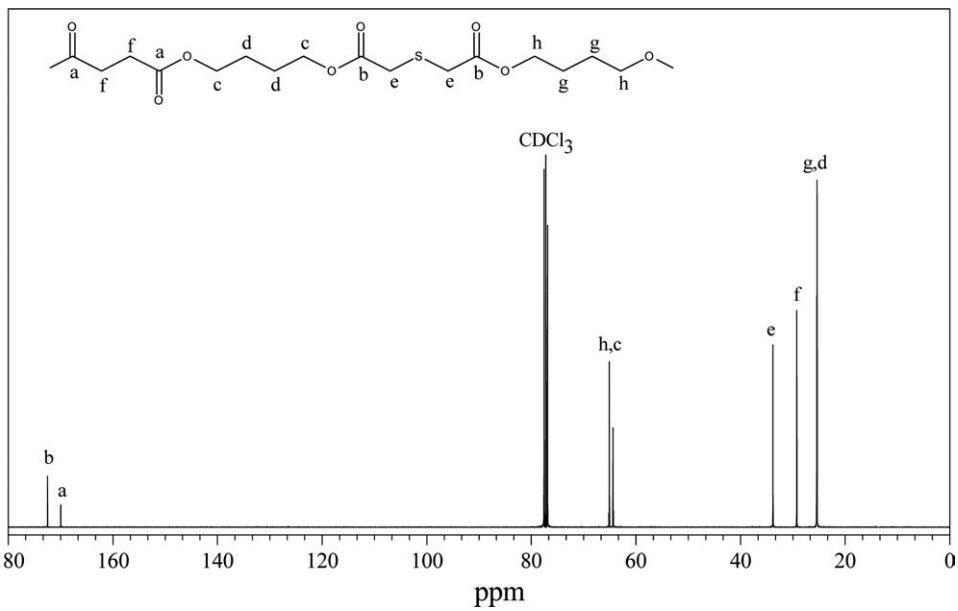

Figure 4 ^{13}C-NMR spectrum of PBSPBTDG120 copolymer.

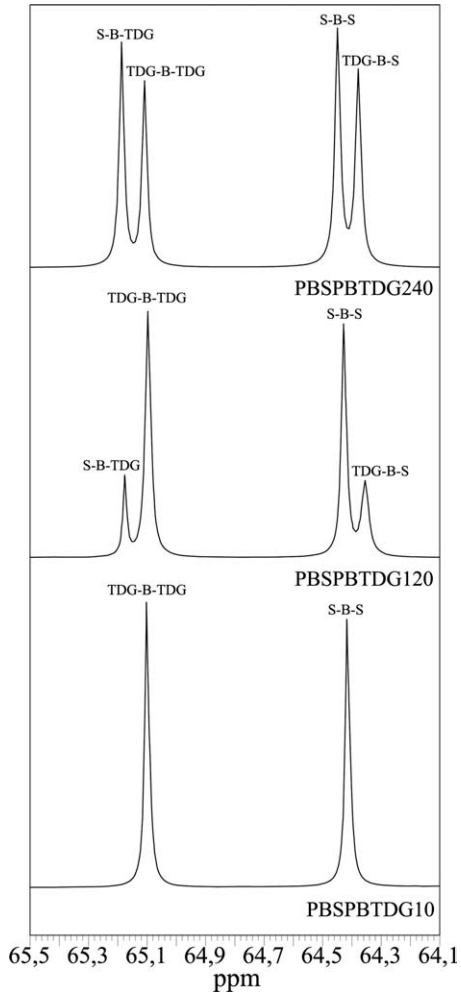

Figure 5 ^{13}C-NMR spectra: expansion of the region between 64.1 and 65.5 ppm. Evolution of the spectrum as a function of mixing time.

$$P_{S-TDG} = \frac{(I_{S-TDG} + I_{TDG-S})/2}{(I_{S-TDG} + I_{TDG-S})/2 + I_{S-S}} \quad (2)$$

$$P_{TDG-S} = \frac{(I_{TDG-S} + I_{S-TDG})/2}{(I_{TDG-S} + I_{S-TDG})/2 + I_{TDG-TDG}} \quad (3)$$

where $I_{S\text{-}TDG}$, $I_{TDG\text{-}S}$, $I_{S\text{-}S,}$ and $I_{TDG\text{-}TDG}$ represent the integrated intensities of the resonance signals of S-TDG, TDG-S, S-S, and TDG-TDG sequences, respectively.

Additionally, the average length of the PBS and PBDG sequences in the copolymer are defined as:

$$L_{BS} = 1/P_{S-TDG} \quad (4)$$

$$L_{BTDG} = 1/P_{TDG-S} \quad (5)$$

The average sequence length for PBS and PBTDG repeated units and the degree of randomness of PBSPBTDG copolyesters are collected in Table I. These results confirmed that the increment of mixing time increases the extent of transesterification reactions. In fact, as these latter proceed, the average length of the PBS and PBTDG sequences decreases and the degree of randomness increases (see Scheme 1 reported below). Therefore, we can conclude that the experimental conditions adopted permitted to prepare several block copolymers, whose block length decreases with the increment of mixing time ($45 < t_{mix} < 180$ min), and lastly a random copolymer (PBSPTDGS240), simply by increasing the reaction time.

The copolyesters were afterwards examined by thermogravimetric analysis and differential scanning calorimetry. The investigation on the thermal stability was carried out under dry nitrogen atmosphere. Analogously to parent homopolymers, the temperature corresponding to 5% weight loss ($T_{5\%}$) and the temperature corresponding to the maximum weight loss rate (T_{max}) were determined from the thermogravimetric curves and collected in Table III.

As it can be seen, the thermal stability of the copolymers is good and very similar to that of PBTDG ($T_{5\%\ w.loss}$ ranging from 322 to 331°C in Table III).

It is well established that the melting behavior of a polymer is affected by its previous thermal history, and therefore, to provide the same heat treatment to all the samples investigated, as mentioned above, before thermal analysis each sample was kept at room temperature for 2 weeks. The DSC traces of the so-treated samples are reported in Figure 6, and the results obtained in Table III. In all cases, a glass transition and a melting phenomenon are evident, with the exception of PBTDG. As far as the glass transition phenomenon is concerned, only one glass transition temperature is always clearly evident, independently of block length, suggesting the presence of a homogeneous amorphous state. Therefore, the melt mixing of the two components for short time ($t_{mix} = 10$ min) favors the miscibility in the amorphous phase even though no significant transesterification reactions took place. The miscibility of the two components in the amorphous phase will be, however, more accurately evaluated analyzing the thermal behavior of the samples after melt quenching (see below).

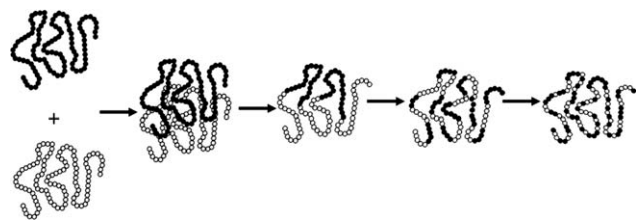

Scheme 1

TABLE III
Thermal Characterization Data of PBS, PBTDG, and PBSPBTDGt Copolymers

			1st Scan				2nd Scan						
Polymers	$T_{5\%\ w.loss}$ (°C)	T_{max} (°C)	T_g (°C)	ΔC_p (J/°C g)	T_m (°C)	ΔH_m (J/g)	T_g (°C)	ΔC_p (J/°C g)	T_c (°C)	ΔH_c (J/g)	T_m (°C)	ΔH_m (J/g)	T_{cc} (°C)
PBS[a]	360	395	−32	0.101	115	81	−34	0.105	/	/	116	64	78
PBDTG	331	366	−48	0.561	/	/	−48	0.577	/	/	/	/	/
PBSPBTDG10	327	381	−40	0.340	113	33	−40	0.348	/	/	113	30	74
PBSPBTDG45	331	374	−40	0.482	100	30	−41	0.526	/	/	99	29	53
PBSPBTDG120	327	380	−41	0.454	79	29	−42	0.423	/	/	79	29	35
PBSPBTDG180	331	376	−41	0.510	58	28	−43	0.604	30	4	64	5	6
PBSPBTDG240	322	379	−41	0.483	50	25	−44	0.628	/	/	/	/	/

[a] From Ref. 15.

Concerning the melting phenomenon from Figure 6, it can be noted that the endothermic process becomes broader and its peak shifts to lower temperature as the mixing time increases. Because PBS crystallizes quite quickly, whereas PBTDG is completely amorphous under the experimental conditions adopted, the melting peaks observed in the copolymers can be attributed to the fusion of the crystalline phase of PBS. Therefore, the decrement of the block length induces the formation of crystals with a low degree of perfection and a wide distribution of dimensions. In fact, the very long blocks of PBS present in PBSPBTDG10 seem to favor the formation of crystals with a good level of perfection [the T_m value (113°C) is in fact very close to that characteristic of the homopolymer (116°C)]. As far as the heat of fusion is concerned, the estimated enthalpy of fusion, after normalization for the butylene succinate unit content, corresponds to 33, 30, 29, 28, and 25% of crystallinity for PBSPBTDG10, PBSPBTDG45, PBSPBTDG120, PBSPBTDG180, and PBSPBTDG240, respectively, assuming 200 J/g as the heat of fusion of perfectly crystalline PBS.[23] Taking into account that PBS homopolymer is characterized by a crystallinity degree of 41%, the presence of noncrystallizable blocks of PBTDG influences the total crystallinity degree of PBS, which crystallizes in the copolymers in minor percentage than in the pure state.

Moreover, in the case of copolymers with short PBS block length (PBSPBTDG45, PBSPBTDG120 and PBSPBTDG180) and the random copolymer (PBSPBTDG240), multiple melting endotherms are evident. Generally speaking, the possible origin of the multiple melting peaks may be listed as follow: (a) presence of more than one crystal structure and (b) melt-recrystallization process occurring during the DSC scan. As well known from the literature, the multiple melting endotherm phenomenon observed in PBS has been ascribed to a reorganization process taking place during the DSC scan, due to a mechanism based on melting and recrystallization of less perfect crystallites into thicker crystals, followed by a final melting process at higher temperature.[24,25] Therefore, the multiple melting peaks present in the DSC traces of the copolymers can be hypothesized to have the same origin.

To investigate more deeply the nature of the crystalline phase in the polymers under investigation, X-ray analysis was performed. The XRD profiles for PBS and PBSPTDGS copolymers are reported in Figure 7. All the samples show the reflections in the angular position characteristic of the α-PBS crystal phase[26]: no extra peaks are present, proving the presence of a unique crystal phase. In the sample PBSPBTDG45, and in PBSPBTDG240, even though only slightly, the intensities of the reflections 020 and 021 are over expressed because of a preferential orientation of the *0 k 0* planes parallel to the

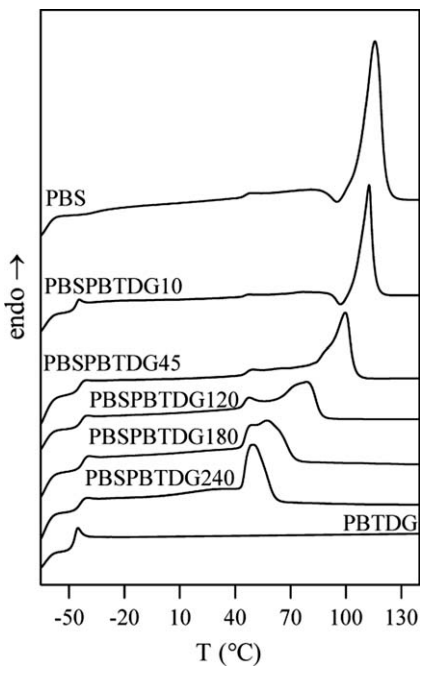

Figure 6 Calorimetric curves of PBS, PBTDG, and their copolymers (1st scan).

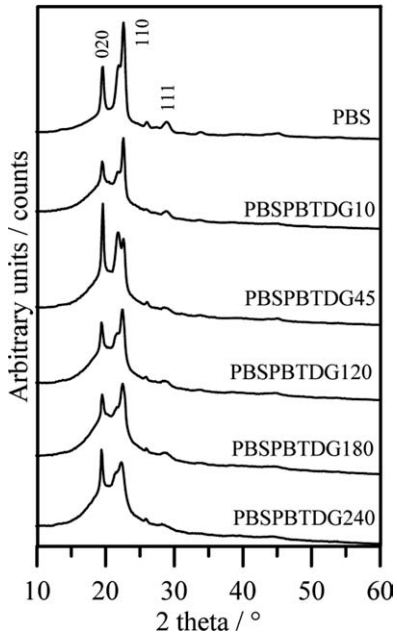

Figure 7 X-ray diffraction patterns of PBS, and PBSPBTDGt copolymers; the indexes of the three main peaks of α-PBS are reported.

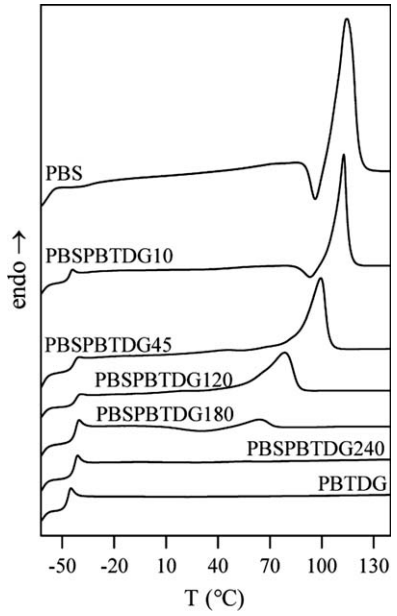

Figure 8 Calorimetric curves of PBS, PBTDG, and PBSPBTDGt copolymers after melt quenching (2nd scan).

sample holder. Unfortunately, XRD analysis carried out in Bragg-Brentano reflection geometry are often affected by this aberration.

Lastly, the overall width of the peaks and the relative area of the halo due the amorphous material increase as the transesterification reactions proceed. Consequently, we can state that the main effect of copolymerization process is an overall worsening of the ordered domains as shown by the decrease of both the crystallinity and the mean crystal size (see Table IV).

The miscibility and the crystallization capacity of PBSPBTDGt samples have been investigated on the samples quenched from the melt (2nd scan). The corresponding DSC traces are shown in Figure 8: as it can be seen, the calorimetric traces of PBS, PBSPBTDG10, PBSPBTDG45, and PBSPBTDG120 are characterized by a glass transition followed by a conspicuous melting endotherm.

TABLE IV
Crystal Sizes in the Direction Perpendicular to 1 1 0 Planes (L_{110}) and Crystallinity Indexes (χ_c)

Polymer	L_{110} (nm)[a]	χ_c (%)
PBS	21(1)	41(4)
PBSPBTDG10	22(1)	33(3)
PBSPBTDG45	22(1)	31(3)
PBSPBTDG120	18(1)	24(3)
PBSPBTDG180	13(1)	20(3)
PBSPBTDG240	12(1)	21(3)

[a] Calculated from the reflection at 19.3° (2θ).

The DSC curve of PBSPBTDG180 shows a glass transition followed by an exothermal "cold crystallization" peak and a melting endotherm at a higher temperature. In particular, the enthalpy of crystallization well compares with the corresponding heat of fusion, indicating that this polymer is completely amorphous. As regards the calorimetric curves of PBSPBTDG240 and pure PBTDG, only an intense endothermal baseline deviation associated with the glass transition is observed. Therefore, the phase behavior of PBSPBTDGt copolymers appears to depend on the mixing time (therefore on the block length): as a matter of fact, after melt quenching, completely amorphous samples can be exclusively obtained at long mixing times.

Regarding the glass transition phenomenon, in all cases only one glass transition is evident, analogously to the first scan, confirming the presence of a single homogeneous amorphous phase. In particular, the PBSPBDGt copolymers obtained at $t_{mix} \geq 180$ min, which, as mentioned above, are completely amorphous after melt quenching, show a glass transition ranging from −43 to −44°C, which well agrees with the value of −44°C predicted by the Fox equation, valid for random copolymers and/or miscible polymer blends (with T_g values of −39 and −48°C for PBS and PBTDG, respectively). In the case of copolymers obtained at $10 \leq t_{mix} \leq 120$ min, slightly higher values of T_g are found (see Table III). This result can be explained on the basis of the higher crystallinity present in these samples.

As far as the melting phenomenon is concerned, an analogous trend to that observed in the first scan was found: the melting point decreases with

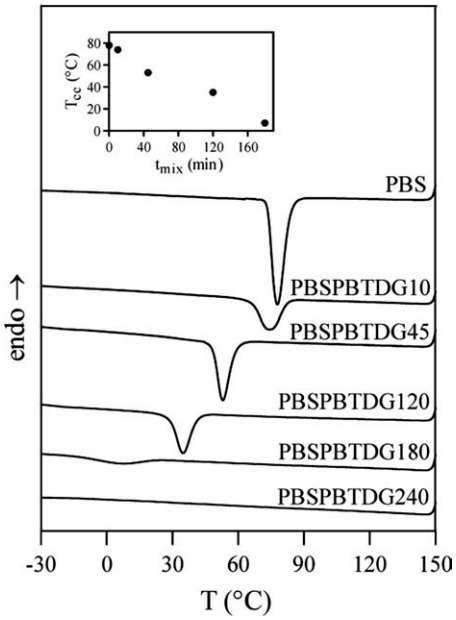

Figure 9 DSC crystallization exotherms of PBS (from Ref. 15) and PBSPBTDGt copolymers cooled from the melt at 5°C/min. In the inset: T_{cc} as a function mixing time.

increasing the mixing time, due to the formation of less perfect crystals; moreover the width of the endothermic peak increases as the mixing time is increased because of the presence of a larger distribution of crystallites with different degree of perfection. Lastly, a decrement of the heat of fusion of the copolymers with respect to that of homopolymer PBS was observed.

To confirm that in the copolymers the tendency of PBS to crystallize decreases, nonisothermal experiments were carried out, subjecting the samples to a controlled cooling rate from the melt (see Experimental Section for details). It is worth remembering that the half-time of primary crystallization in isothermal experiments correlates with the temperature corresponding to the maximum of the crystallization peak in nonisothermal experiments (T_{cc}),[27] being this latter more easily obtainable. The exothermic crystallization peaks of the samples under investigation are displayed in Figure 9: as it can be seen, the copolymers obtained at mixing times longer than 180 min are not able to crystallize even though cooled from the melt at very low rate (1°C/min). From the inset of Figure 9, where the T_{cc} values are reported as a function of mixing time, it can be observed that the temperature corresponding to the maximum of the exothermal crystallization peak regularly decreases as the mixing time is increased.

This result indicates that the crystallization process becomes more and more difficult as the PBS blocks become progressively shorter, and the copolymer tends toward a random distribution of the sequences. Such trend is due to the effect of the

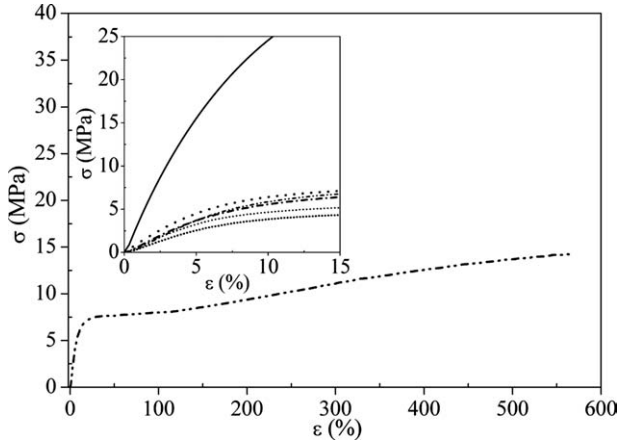

Figure 10 Stress–strain curve of PBSPBTDG120. In the inset: enlarged zone of the initial linear portion of the stress–strain curve: solid line PBS; dot PBSPBTDG10; dash dot PBSPBTDG45; dash dot dot PBSPBTDG120; short dash PBSPBTDG180; short dot PBSPBTDG240.

PBTDG phase, which limits the transport of the PBS chains on the crystal surface and act as a defect during chain folding. Therefore, in block copolymers, a decrement of the crystallization rate with a reduction of the block length is evident.

Taking into account that strain affects stem cells biology, the investigation of mechanical properties of PBSPBTDGt copolymers is crucial. The tensile behavior of the investigated polymers, together with that of PBS added for comparison, is shown in Figure 10 that plots, as an example, the stress as a function of strain for PBSPBTDG120. Table V reports the corresponding mechanical characteristics (elastic modulus, E; stress at break, σ_b, and deformation at break, ε_b), together with those of PBS, and some of the copolymers PBSPBDG previously investigated.[15]

As it can be seen, all the copolymers are characterized by a lower elastic modulus and, therefore, are less strong in comparison with PBS. Moreover, elastic modulus and elongation to break decreases and increases, respectively, as the block length decreases. Since all the investigated polymers display a soft amorphous phase (T_g values are in all cases well

TABLE V
Mechanical Data of PBS, PBSPBTDGt, and PBSPBDGt (from Ref. 15) Copolymers

Polymers	E (MPa)	ε_b (%)	σ_b (MPa)
PBS	337 ± 26	24 ± 4	31 ± 2
PBSPBTDG10	160 ± 15	95 ± 4	18 ± 1
PBSPBTDG45	87 ± 8	464 ± 82	12 ± 2
PBSPBTDG120	86 ± 2	510 ± 95	13 2
PBSPBTDG180	75 ± 5	610 ± 16	11± 1
PBSPBTDG240	61 ± 4	713 ± 51	7 ± 1
PBSPBDG5	229 ± 20	17 ± 1	18 ± 1.5
PBSPBDG90	101 ± 8	773 ± 24	16 ± 1
PBSPBDG180	83 ± 7	883 ± 72	16 ± 2.5

below RT), the observed trend can be ascribed to the decrease in crystallinity degree (see Table IV).

The copolymers PBSPBTDGX obtained at $t_{mix} \geq$ 45 min are characterized by an elastomeric behavior, which is particularly important in the context of soft tissue engineering applications. Quite interesting is the comparison with the PBSPBDG copolymers previously investigated.[15] PBSPBDG5, PBSPBDG90, and PBSPBDG180 are characterized by practically same block length and by the same crystallinty degree compared to PBSPBTDG10, PBSPBTDGS180, and PBSPBTDG240, respectively. Nevertheless, the sulfur-containing copolymers are less rigid than the corresponding ethero-atom containing samples (E decreases of 25% and ε_b increases of 20%). This result can be correlated to the higher chain flexibility of PBSPBTDG copolymers on respect to PBSPBDG ones, due to the presence along the polymeric chain of C—S bonds longer than the C—O ones and to weaker interchain interactions because of the lower electronegativity of sulfur atoms with respect to oxygen ones.

CONCLUSIONS

The ScbPBS-PBTDG blends are immiscible when physically blended, as proved by the presence of two T_g temperatures. By heating the blends at high temperature (225°C), the original two amorphous phases merged into one single phase, proving that chemical reactions induced amorphous phase homogenization. The PBSPBTDG copolymers were prepared via a simple and straightforward method, i.e., reactive blending. As a matter of fact, NMR data and the DSC results indicate that either block copolymers with well-defined length, which decreases with increasing mixing time, or random copolymers can be easily obtained. A detailed investigation of thermo-mechanical properties of copolymers allowed to correlate copolymer properties to its specific molecular architecture. In particular, it has been demonstrated that the introduction of BTDG units into PBS chain has the effect of tailoring polymer mechanical properties (as a consequence of the depression of polymer crystallinity degree) toward an elastomeric behavior, which is particularly important in the context of soft tissue engineering applications.

Obviously, further steps of the research concerning the investigation of biodegradability, biocompatibility, and processability through scaffold-manufacturing techniques are important to confirm the potential utilization of these new copolyesters in soft tissue engineering field.

References

1. Serrano, M. C.; Chung, E. J.; Ameer, G. A. Adv Funct Mater 2010, 20, 192.
2. Guelcher, S. A. Tissue Eng B 2008, 14, 3.
3. Hong, Y.; Guan, J.; Fujimoto, K. L.; Hashizume, R.; Pelinescu, A. L.; Wagner, W. R. Biomaterials 2010, 31, 4249.
4. Pego, A. P.; Poot, A. A.; Grijpma, D. W.; Feijen, J. J Controlled Release 2003, 87, 69.
5. Pego, A. P.; Siebum, B.; Luyn, V.; Gallego, X. J.; Seijen, Y. V.; Poot, A. A.; Grijpma, D. W.; Feijen, J. Tissue Eng 2003, 9, 981.
6. Ozawa, T.; Mickle, D. A. G.; Weisel, R. D.; Koyama, N.; Ozawa, S.; Li, R-K. Circulation 2002, 106, I.
7. Bruggeman, J. P.; De Bruin, B-J.; Bettinger, C. J.; Langer, R. Biomaterials 2008, 29, 4726.
8. Wang, Y.; Ameer, G. A.; Sheppard, B. J.; Langer, R. Nat Biotechnol 2002, 20, 602.
9. Soccio, M.; Lotti, N.; Finelli, L.; Gazzano, M.; Munari, A. Eur Polym J 2008, 44, 1722.
10. Soccio, M.; Lotti, N.; Finelli, L.; Munari, A. Eur Polym J 2009, 45, 171.
11. Gualandi, C.; Soccio, M.; Govoni, M.; Valente, S.; Lotti, N.; Munari, A.; Giordano, E.; Pasquinelli, G.; Focarete, M. L. J Bioact Compat Polym, to appear.
12. Soccio, M.; Lotti, N.; Gigli, M.; Finelli, L.; Gazzano, M.; Munari, A. Polym Int, to appear.
13. Soccio M.; Lotti N.; Gazzano M.; Govoni M.; Giordano E.; Munari A. Biomacromolecules, submitted.
14. Gualandi, C.; Soccio, M.; Saino, E.; Focarete, M. L.; Lotti, N.; Munari, A.; Moroni, L.; Visai, L. Soft Matter, submitted.
15. Gigli, M.; Lotti, N.; Gazzano, M.; Finelli, L.; Munari, A. Polym Eng Sci, submitted.
16. Marchese, P.; Celli, A.; Fiorini, M. Macromol Chem Phys 2002, 203, 695.
17. Okamoto, M.; Kotaka, T. Polymer 1997, 38, 1357.
18. Aoki, Y.; Li, L.; Amari, T.; Nishimura, K.; Arashiro, Y. Macromolecules 1999, 32, 1923.
19. Khonakdar, H. A.; Golriz, M.; Jafari, S. H.; Wagenknecht, U. Macromol Mater Eng 2009, 294, 272.
20. Klug, H. P.; Alexander, L. E. X-ray Diffraction Procedures for Polycrystalline and Amorphous Materials, 2nd ed.; Wiley-Interscience: New York, 1974.
21. Zimmermann, H. In Developments in Polymer Degradation; Grassie, N., Ed.; Applied Science Publishers: London, 1984; Vol. 5, p 79.
22. Chen, M. S.; Chang, S. J.; Chang, R. S.; Kuo, W. F.; Tsai, H. B. J Appl Polym Sci 1990, 40, 1053.
23. Hexig, B.; Alata, H.; Asakawa, N.; Inoue, Y. J Polym Sci Part B: Polym Phys 2005, 43, 368.
24. Yoo, E. S.; Im, S. S. J Polym Sci Polym Phys 1999, 37, 1357.
25. Yasuniwa, M.; Tsubakihara, S.; Satou, T.; Iura, K. J. J Polym Sci Part B: Polym Phys 2002, 40, 2411.
26. Ichikawa, Y.; Kondo, H.; Igarashi, Y.; Noguchi, K.; Okuyama, K.; Washiyama, J. Polymer 2000, 41, 4719; Ichikawa, Y.; Kondo, H.; Igarashi, Y.; Noguchi, K.; Okuyama, K.; Washiyama, J. Corrigendum Polymer 2001, 42, 847.
27. Legras, R.; Dekoninck, J. M.; Vanzieleghem, A.; Mercier, J. P.; Nield, E. Polymer 1986, 27, 109.